

# UC San Diego

## UC San Diego Previously Published Works

**Title**

Ablation of Cypher, a PDZ-LIM domain Z-line protein, causes a severe form of congenital myopathy.

**Permalink**

<https://escholarship.org/uc/item/6jm8c8qh>

**Journal**

The Journal of cell biology, 155(4)

**ISSN**

0021-9525

**Authors**

Zhou, Q  
Chu, PH  
Huang, C  
et al.

**Publication Date**

2001-11-01

**DOI**

10.1083/jcb.200107092

Peer reviewed

# Ablation of Cypher, a PDZ-LIM domain Z-line protein, causes a severe form of congenital myopathy

Qiang Zhou,<sup>1</sup> Po-Hsien Chu,<sup>1</sup> Chenqun Huang,<sup>1</sup> Ching-Feng Cheng,<sup>1</sup> Maryann E. Martone,<sup>2</sup> Gudrun Knoll,<sup>1</sup> G. Diane Shelton,<sup>3</sup> Sylvia Evans,<sup>1</sup> and Ju Chen<sup>1</sup>

<sup>1</sup>Institute of Molecular Medicine and Department of Medicine, <sup>2</sup>Department of Neuroscience, and <sup>3</sup>Department of Pathology, University of California at San Diego School of Medicine, La Jolla, CA 92093

**C**yper is a member of a recently emerging family of proteins containing a PDZ domain at their NH<sub>2</sub> terminus and one or three LIM domains at their COOH terminus. *Cypher* knockout mice display a severe form of congenital myopathy and die postnatally from functional failure in multiple striated muscles. Examination of striated muscle from the mutants revealed that Cypher is

not required for sarcomerogenesis or Z-line assembly, but rather is required for maintenance of the Z-line during muscle function. In vitro studies demonstrated that individual domains within Cypher localize independently to the Z-line via interactions with  $\alpha$ -actinin or other Z-line components. These results suggest that Cypher functions as a linker-strut to maintain cytoskeletal structure during contraction.

## Introduction

We have recently described a novel protein, Cypher, which is a member of a newly emerging group of cytoskeletal proteins containing one NH<sub>2</sub>-terminal PDZ domain, and one or three COOH-terminal LIM domains. Within this family, Enigma, ENH, and Cypher/ZASP contain three COOH-terminal LIM domains; and Ril, CLP 36/HCLIM1, and actinin-associated LIM protein (ALP)\* contain one (Wu and Gill, 1994; Kiess et al., 1995; Wang et al., 1995; Kuroda et al., 1996; Xia et al., 1997; Faulkner et al., 1999; Zhou et al., 1999). All six members have been shown to associate with the cytoskeleton, five of them via interactions with  $\alpha$ -actinin and/or  $\beta$ -tropomyosin. The functional role of any of these proteins is largely unknown.

We have identified two distinct splice variants of Cypher, designated Cypher1 and Cypher2. Both isoforms are expressed exclusively in striated muscle at significant levels from embryonic development into adulthood, and are localized to the Z-line (Zhou et al., 1999). The Cypher1 isoform contains a PDZ domain at its NH<sub>2</sub> terminus, three LIM domains at its COOH terminus, and nine 'YS/TPS/TP' amino acid repeats. Of these domains, Cypher2 shares only the

PDZ domain. Consistent with their localization at the Z-line, both Cypher isoforms can bind to  $\alpha$ -actinin 2 through their PDZ domain (Zhou et al., 1999).  $\alpha$ -Actinin 2, a striated muscle-specific  $\alpha$ -actinin that contains an NH<sub>2</sub>-terminal actin-binding domain, four central spectrin-like repeats, and four COOH-terminal regions homologous to calcium-binding EF hands, is a major component of the Z-line of striated muscle (Beggs et al., 1992; Young et al., 1998; Djinnovic-Carugo et al., 1999).

The role that Cypher might play in Z-line formation or function is unknown. The Z-line, alternatively termed the Z-band or Z-disc, is an electron-dense structure which is the interface from sarcomere to sarcomere and from myofibril to myofibril. The Z-band also represents the convergence of a number of protein complexes important for sarcomeric-cytoskeletal extracellular matrix interactions (Goldstein et al., 1991; Luther, 2000). Despite the knowledge we have about the existence of these complexes, mechanisms of complex formation and their specific requirement for muscle function remain largely unknown.

This manuscript describes in vivo and in vitro studies we have recently performed which give insight into the biological functions of Cypher. Analysis of striated muscles from Cypher mutant mice suggested that Cypher is not required for sarcomerogenesis or Z-line formation, but rather is essential to support Z-line structure and muscle function during contraction. In concert with our in vitro data demonstrating that Cypher interacts with  $\alpha$ -actinin and at least one other Z-line component, our data suggest a model in which Cypher serves as an essential linker-strut to reinforce protein interactions at the Z-line.

Address correspondence to Ju Chen, Department of Medicine, University of California at San Diego School of Medicine, 9500 Gilman Dr., La Jolla, CA 92093-0613. Tel.: (858) 822-2452. Fax: (858) 534-2069. E-mail: juchen@ucsd.edu

\*Abbreviations used in this paper: aa, amino acid; ALP, actinin-associated LIM protein; E, embryonic day; GFP, green fluorescent protein; TEM, transmission electron microscopy.

Key words: congenital myopathy; cypher; LIM; PDZ; Z-line

## Results

### Ablation of Cypher (both Cypher1 and Cypher2) in mouse results in perinatal lethality

To understand the *in vivo* function of Cypher in striated muscle and to exploit *cypher* as a potentially useful lineage marker, we used homologous recombination to knock-in a  $\beta$ -galactosidase cDNA downstream of the endogenous *cypher* promoter, meanwhile disrupting the *cypher* gene which encodes both Cypher1 and Cypher2 (Fig. 1). Assays for  $\beta$ -galactosidase activity are very sensitive and give resolution at the single cell level, thus permitting us to look in greater detail at expression of *cypher* during embryogenesis (Chu et al., 2000). As shown in Fig. 2, *cypher* is expressed exclusively in heart at embryonic day (E) 8.5, but at E 9.5 it was detected in somites in a rostral to caudal gradient, with highest expression rostrally. The somite expression pattern progresses caudally through E 11.5, corresponding to somite maturation. At this stage, *cypher* expression was also detected in cells migrating from the myotome. At E 13.5, *cypher* expression was detected throughout the embryonic musculature. The X-gal staining pattern observed here matches well with our previous RNA in situ hybridization results, with the exception that the X-gal staining was observed earlier in the somites, in keeping with its greater sensitivity (Zhou et al., 1999).

No viable *cypher*<sup>-/-</sup> mutants were obtained in litters from *cypher*<sup>+/-</sup> intercrosses at weaning, indicating that the *cypher* null mutation was embryonic or perinatal lethal. Analysis of

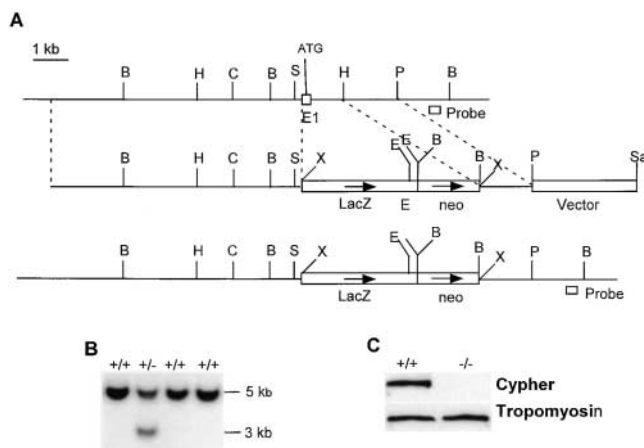


**Figure 1. Targeting the *cypher* gene.** (A) Targeting strategy. A restriction map of the relevant genomic region of *cypher* is shown on top, the targeting construct is shown in the center, and the mutated locus after recombination is shown at the bottom. ATG is the translational start site. The arrow indicates the orientation of  $\beta$ -galactosidase cDNA and neomycin resistance gene. B, BamHI; C, ClaI; E, EcoRI; H, HindIII; P, PstI; S, SstI; Sa, SalI; X, XbaI.  $\beta$ -Galactosidase cDNA; and neo, neomycin resistance gene. (B) Detection of wild-type and targeted alleles by Southern blot analysis. DNAs from electroporated ES cells were digested with BamHI and analyzed by Southern blot analysis with probe as shown in A. The 5- and 3-kb bands represent wild-type and targeted allele, respectively. (C) Detection of Cypher protein by Western blot analysis. Proteins prepared from neonatal day 1 skeletal muscle of wild-type (+/+) and *cypher* knockout mice (-/-) were analyzed with anti-Cypher (top) and antitropomyosin C monoclonal antibodies (bottom).

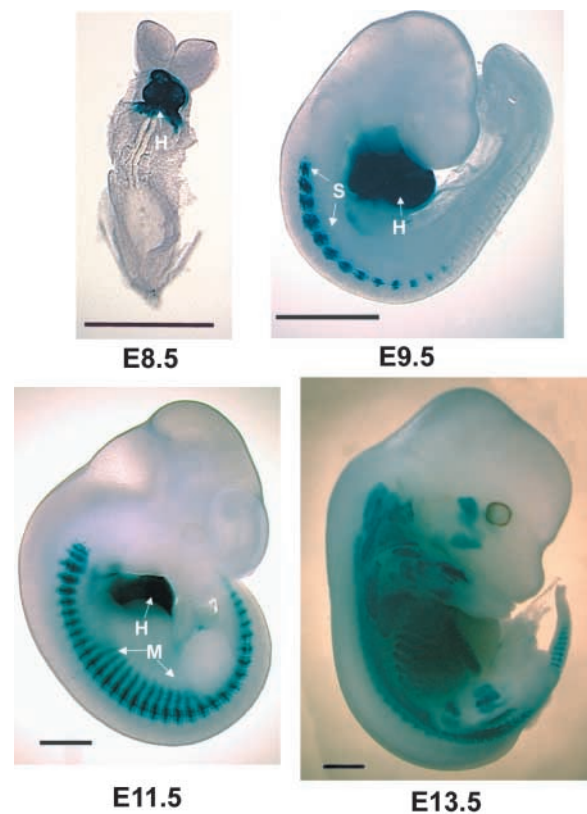


**Figure 2. X-gal staining of *cypher* LacZ/knock-in heterozygous embryos at different development stages.** Embryos from embryonic day (E) 8.5, 9.5, 11.5, and 13.5 were stained with X-gal for ~8 h at 30°C. X-gal staining of heart (H) was detected from E 8.5. Somite (S) staining was not detectable at E 8.5, but was detected at E 9.5 in a decreasing rostral to caudal gradient. The somite expression pattern progresses caudally through E 11.5, corresponding to somite maturation. At this stage, *cypher* expression was also detected in cells migrating from the myotome (M). At E 13.5, *cypher* expression was detected throughout the embryonic musculature. Bar, 1 mm.

99 newborn mice from 10 independent heterozygous crosses indicated that 29 were homozygous knock-out for *cypher*, approximating the expected frequency of 25%. These data indicated that ablation of *cypher* was perinatal lethal. To verify that homozygous knockout mice were null mutants, we performed Western blot analyses for Cypher protein. As shown in Fig. 1 C, no Cypher protein was detected in homozygous mutant mice.

### *Cypher*<sup>-/-</sup> mutants die from functional failure in multiple striated muscle types

The majority of *cypher*<sup>-/-</sup> mice died within 24 h of birth. Some null mutants died immediately after birth, while others survived from 2 to 5 d postnatally. None of the *cypher* null mutants survived beyond day five. All mutants were cyanotic, some with a gasping respiratory pattern. The mutants also displayed limb weakness, exhibiting a limited range of motion. No obvious body weight differences were found at birth between mutant and wild-type or heterozygous mice. Subsequently, little or no milk was detected in the stomach of homozygous null mutants, presumably a reflection of their inability to suckle. Consistent with this ob-

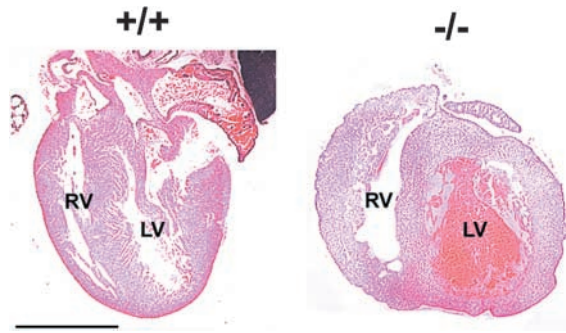


Figure 3. **Histological analyses of skeletal and cardiac muscles from *cypher*<sup>-/-</sup> and their wild-type littermate controls.** Sagittal sections of postnatal day 1 wild-type (+/+) and *cypher* knockout mice (-/-) were stained with hematoxylin and eosin. Note the ventricular dilation in the knockout mice. RV, right ventricle; LV, left ventricle. Bar, 1 mm.

servation, null mutants had no significant postnatal gain in body weight and exhibited minimal subcutaneous fat.

Sections of skeletal muscle and heart from postnatal day 1 *cypher*<sup>-/-</sup> mutants and wild-type littermate controls were prepared and examined by light microscopy. At this level of resolution, no significant differences were observed in skeletal muscle from the two groups (unpublished data). However, examination of hearts from homozygous mutant ani-

mals revealed blood congestion and dilation of both right and left ventricles (Fig. 3).

To determine whether ablation of Cypher had affected other cytoskeletal proteins, we performed immunostaining analyses of neonatal skeletal muscle for a number of proteins representing diverse components of the cytoskeleton including  $\alpha$ -actinin 2 and desmin; sarcomeric proteins myosin heavy chain and tropomyosin; and the extrasarcomeric protein vinculin. No significant differences were found between homozygous mutant and wild-type control mice (unpublished data).

### ***Cypher*<sup>-/-</sup> skeletal and cardiac muscle display disorganized and fragmented Z-lines**

Ultrastructural transmission electron microscopy (TEM) analysis was performed on comparable areas of skeletal muscle from day 1 wild-type and mutant mice. Intercostal, thigh, and diaphragm muscles were examined. Of these, the most severely affected was diaphragm muscle. A comparison of diaphragm muscle from day 1 wild-type and mutant mice revealed severely disorganized and disrupted Z-lines in the mutant muscle, with relatively normal M-lines (Fig. 4, C and D).

To determine whether abnormal Z-line structure resulted from defects in the initial assembly of protein complexes at the Z-line, and/or an inability to maintain Z-line integrity during muscle function, ultrastructural TEM analysis was

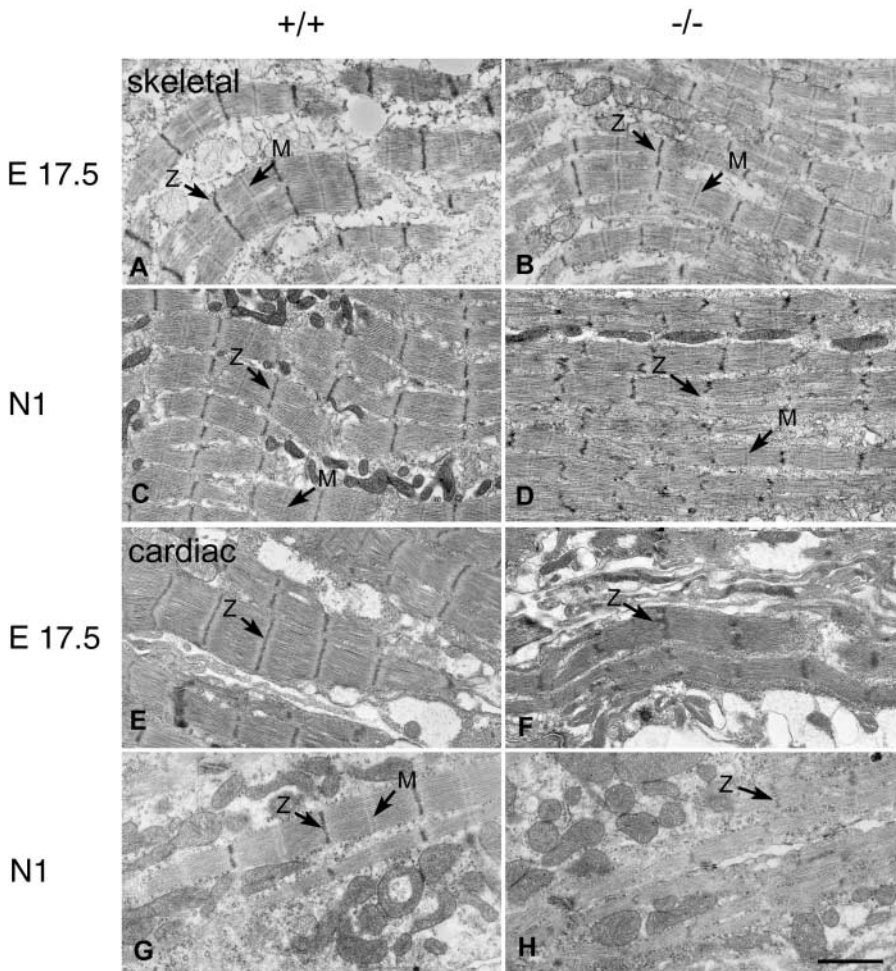
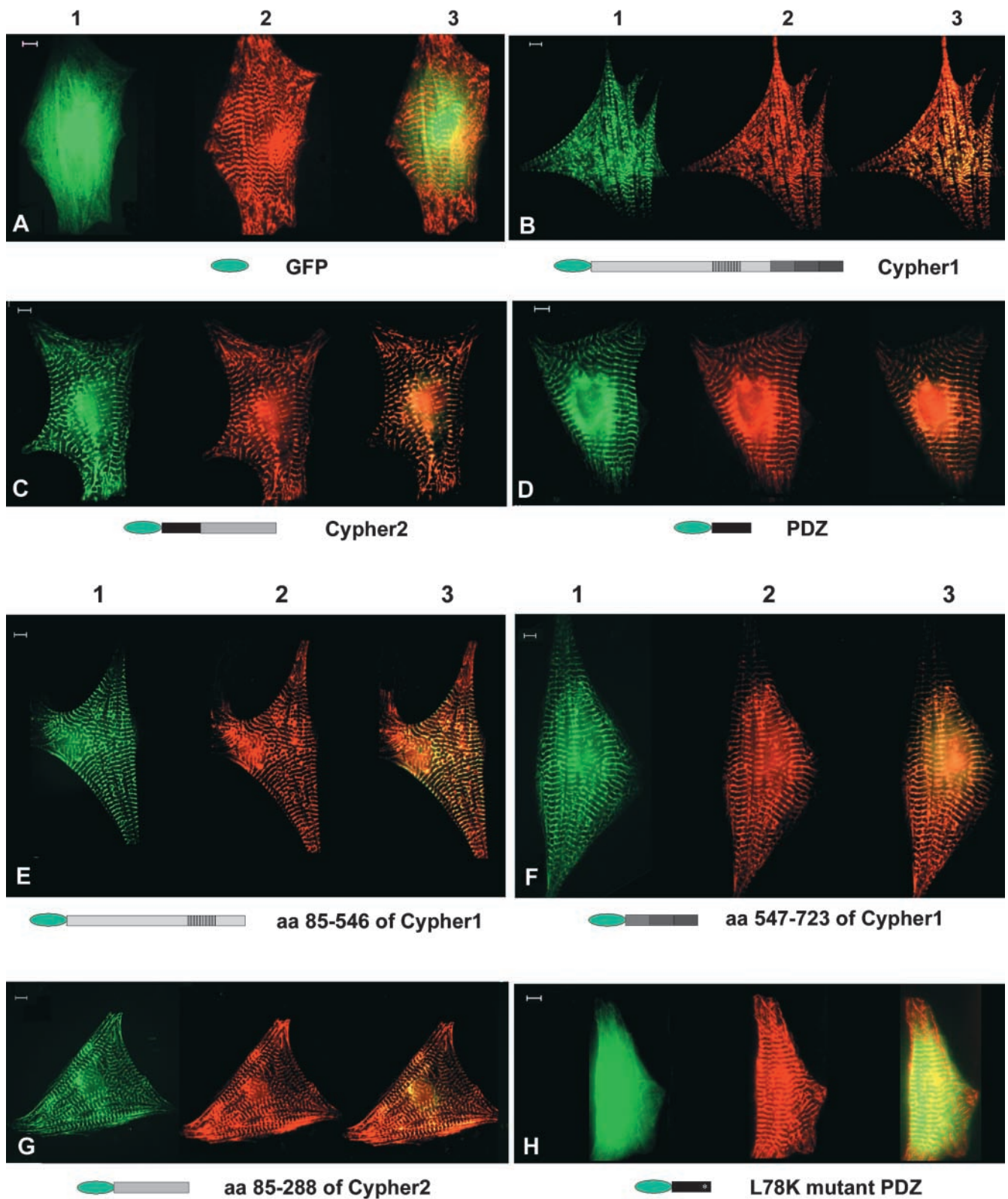


Figure 4. **Ultrastructural analysis of diaphragm muscle and heart architecture as assessed by TEM.** Representative images from diaphragm muscle of E 17.5 and day 1 neonatal (N1) wild-type (+/+) and *cypher* knockout (-/-) mice (A–D). A comparison of diaphragm muscle from wild-type and knockout mice at E 17.5, when diaphragm muscle is inactive, shows well-preserved Z-line and M line structure (A and B). In contrast, Z-lines in diaphragm muscle from knockout mice at postnatal day 1 are severely disorganized and disrupted; M-lines, however, are relatively normal (C and D). Representative images from cardiac muscle of E 17.5 and day 1 neonatal wild-type and *cypher* knockout mice (E–H). In embryonic cardiac muscle, Z lines are evident, but distinct, well-formed M lines are not yet present (Anversa et al., 1981). In *Cypher* knockout mice, E 17.5 cardiac muscle, which has been functional since E 8, exhibits fragmented and disorganized Z-lines (E and F). In postnatal day 1 cardiac muscle of wild-type mice, both Z-lines and M-lines are well formed and distinctly visible. In contrast, only remnants of the Z-line and no M-lines are visible in cardiac muscle from mutant mice (G and H). Bar, 1.5  $\mu$ m.





**Figure 5. Fluorescence microscopy of neonatal rat cardiomyocytes transfected with GFP fusions of distinct Cypher domains.** Transfected rat neonatal cardiomyocytes were stained after 2 d in culture: lane 1, GFP fusion proteins (green); lane 2, rhodamine staining for  $\alpha$ -actinin 2 (red); lane 3, superimposition of the two images (orange). (A) GFP alone; (B) Cypher1; (C) Cypher2; (D) PDZ domain (aa 1-84 of Cypher); (E) YS/TPS/TP repeat-containing region (aa 85-546 of Cypher1); (F) LIM domains (aa 547-723 of Cypher1); (G) PDZ-less Cypher2 (aa 85-288 of Cypher2); and (H) L78K mutant PDZ domain. Each distinct domain of Cypher1 and Cypher2, including the PDZ domain, independently localized to the Z-line (B-G). Disruption of  $\alpha$ -actinin 2 binding by mutation of L78K within the Cypher PDZ domain prevented exclusive localization to the Z-line (H). Bar, 10  $\mu$ m.

performed on comparable areas from diaphragm muscle of mutant and wild-type mice at E 17.5. Diaphragm muscle does not contract until birth. If Cypher is required for formation of protein complexes at the Z-line and/or sarcomerogenesis, rather than to sustain Z-line structure during contraction, we would expect to observe abnormal Z-line structure and/or abnormal sarcomeric structure in noncontracting embryonic diaphragm muscle. At E 17.5, diaphragm muscle from wild-type and mutant mice was virtually indistinguishable, with intact and well-organized Z-lines and M-lines (Fig. 4, A and B). However, at postnatal day 1, after active contraction of the diaphragm, there was a striking difference between wild-type and mutant muscle (Fig. 4, C and D).

We also performed ultrastructural analysis of cardiac muscle from E 17.5 and postnatal day 1 wild-type and mutant mice (Fig. 4, E–H). In contrast to diaphragm muscle, cardiac muscle begins to contract at E 8. Therefore, E 17.5 muscle has been actively contracting for some time. An examination of cardiac muscle from E 17.5 revealed that cypher knockout tissue exhibited fragmented and disorganized Z-lines (Fig. 4, E and F). At this stage, M-lines are not fully developed in cardiac muscle (Anversa et al., 1981). Examination of cardiac muscle from postnatal day 1 mice revealed complete absence of Z- or M-lines in muscle from mutant mice (Fig. 4, G and H). In knockout mice, M-line perturbation in postnatal day 1 cardiac muscle is likely to be secondary to prolonged muscle malfunction after Z-line perturbation, as postnatal day 1 diaphragm muscle which has recently begun to contract and display abnormal Z-lines has relatively normal M-lines.

These results obtained in Cypher knockout mice demonstrate that Cypher is essential to striated muscle function, and suggest that it is required for the maintenance of Z-line structure during contraction, rather than initial formation of the Z-line. To gain further insight into the biochemical functions and mechanisms by which Cypher achieves this role, we performed a number of *in vitro* studies to further address Cypher function.

### Distinct non-PDZ domains of Cypher1 or Cypher2 independently localize to the Z-line

The phenotype of *cypher* null mutant mice suggested that Cypher is essential for maintaining Z-line structure. One potential mechanism by which Cypher could be performing this function is to act as a linker between  $\alpha$ -actinin and other Z-line components, thus reinforcing Z-line structure. Our previous data have shown that the non-PDZ domains of cypher do not interact with  $\alpha$ -actinin. Do they, however, interact with other Z-line components? To investigate this possibility, we determined the localization of each non-PDZ domain in cultured neonatal rat cardiomyocytes. A cDNA encoding green fluorescent protein (GFP) was fused to full-length Cypher1, Cypher2, and each distinct domain within these Cypher proteins. A GFP fusion construct was also made for a mutant PDZ domain which no longer binds to  $\alpha$ -actinin 2 (L78K; see Fig. 6). Resulting constructs were then transfected into rat neonatal cardiomyocytes. 2 d after transfection, cells were immunostained with anti- $\alpha$ -actinin 2 antibody. Antibody staining and GFP expression were visualized by fluorescence microscopy (Fig. 5).

Results of these studies demonstrated that control GFP was localized diffusely throughout the cell. In contrast, each distinct non-PDZ domain of Cypher1 or Cypher2 colocalized with  $\alpha$ -actinin 2 at the Z-line (Fig. 5, B–G). The mutant PDZ (L78K)–GFP fusion did not localize to the Z-line, but rather was distributed diffusely throughout the cell (Fig. 5 H).

### Mutations in the PDZ domain disrupt interaction with $\alpha$ -actinin 2

We have shown previously that both Cypher1 and Cypher 2 bind to  $\alpha$ -actinin 2 through their PDZ domains. To determine which amino acids within the PDZ domain are essential for interaction with  $\alpha$ -actinin 2, we introduced mutations within the PDZ domain via PCR-based mutagenesis. Mutant PDZ domains, and a control wild-type PDZ domain were fused to GST, and pull-down assays were performed to evaluate the interaction between mutant PDZ domains and  $\alpha$ -actinin 2.

The mutant amino acids were chosen according to the crystal structure of the PDZ-3 domain of PSD-95 (Doyle et al., 1996) and studies of the ALP PDZ domain (Xia et al., 1997). Interactions between PDZ3 of PSD-95 and target peptide side chains suggest that the amide nitrogens within a GLGF motif of PDZ3 play an important role in forming hydrogen bonds with the COOH terminus of the target peptide. Alignment of the Cypher PDZ and PDZ3 of PSD-95 reveal a PWGF (amino acids [aa] 11–14) sequence within the Cypher PDZ at the position corresponding to GLGF within PDZ3. As shown in Fig. 6, mutation of the PWGF motif (G14A/F15A) within Cypher PDZ domain disrupted binding to  $\alpha$ -actinin 2. We have also performed GFP fusion cell localization studies with this mutant, and confirmed that it no longer localizes to the Z-line, but rather is distributed diffusely, as seen with mutant L78K (unpublished data).

The crystal structure also indicates that a histidine residue within the  $\alpha$ B region of PDZ3 of PSD-95 is critical for the formation of a hydrogen bond with the target peptide (Songyang et al., 1997). Mutation of the analogous histidine within the Cypher PDZ domain (H62A) had no significant effect on interaction between the Cypher PDZ and  $\alpha$ -actinin 2 (Fig. 6).

It has been shown that mutation of L78 to K78 in the ALP PDZ domain abolishes the interaction of ALP with

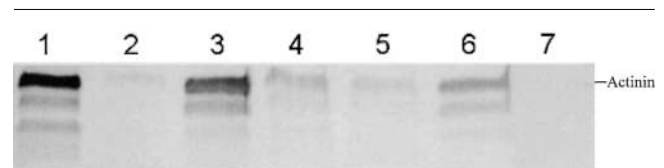
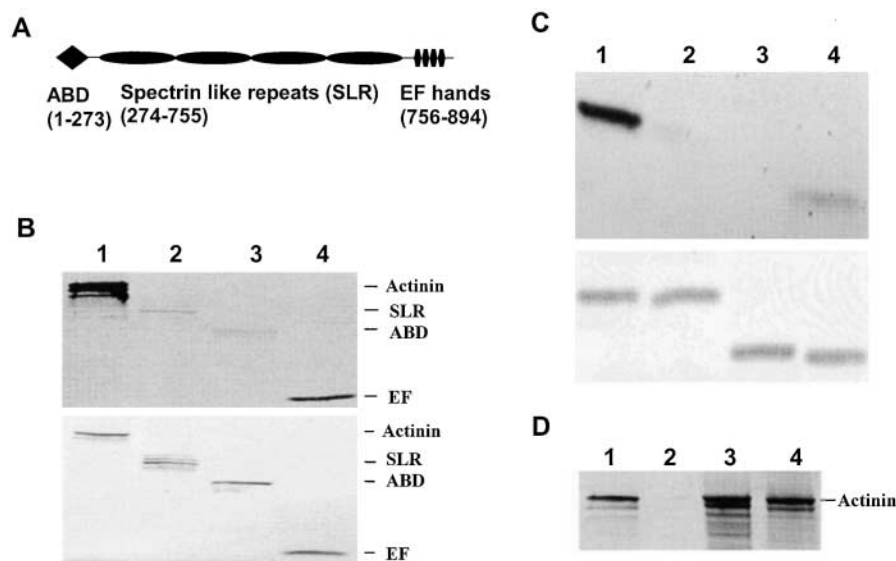


**Figure 6. Interaction assays of wild-type and mutant GST-PDZ fragments and radiolabeled  $\alpha$ -actinin 2.** Autoradiogram [ $^{35}$ S]methionine-labeled full-length  $\alpha$ -actinin 2 after incubation and precipitation with the following GST-PDZ fragments: lane 1, GST–wild-type PDZ; lane 2, GST–G14A/W15A PDZ; lane 3, GST–H62A PDZ; lane 4, GST–L76K PDZ; lane 5, GST–L78K PDZ; lane 6, GST–L80K PDZ; lane 7, GST control. All incubations included equal amounts of input  $\alpha$ -actinin 2. Mutation of G14A/W15A or L76K within the PDZ domain abolished binding to  $\alpha$ -actinin 2. Exposure time for the autoradiogram was 5 h at room temperature.

**Figure 7. Interaction of the PDZ domain of Cypher requires the COOH terminus of  $\alpha$ -actinin.**

(A) Schematic diagram of  $\alpha$ -actinin 2. The actin binding domain (ABD, aa 1–273), spectrin-like repeats (SLR, aa 274–755), and EF hands (aa 756–894) are indicated. B. Autoradiogram of  $^{35}\text{S}$  methionine-labeled proteins after coprecipitated with GST-PDZ glutathione resin (see Materials and Methods). Lane 1, full-length  $\alpha$ -actinin 2; lane 2, Spectrin repeats; lane 3, ABD domain; lane 4, the four EF hands. Exposure time for the autoradiogram was 4 h at room temperature. The bottom panel shows the input of each in vitro translated protein. Exposure time for the autoradiogram was 20 min at room temperature. Strongest binding to the PDZ domain was observed with the COOH-terminal four EF hands of  $\alpha$ -actinin 2 (lane 4). C. Autoradiogram of  $^{35}\text{S}$  methionine-labeled  $\alpha$ -actinin 2 COOH-terminal fragments after coincubation and precipitation with GST-PDZ fusion proteins. Lane 1,  $^{35}\text{S}$ -labeled four EF hands (4EF, aa 756 to 894); lane 2, four EF hands deleted for the three COOH-terminal amino acids (4EF-del3, aa 756 to 891); lane 3, first two EF hands (EF1–2, aa 756–821); lane 4, last two EF hands (EF3–4, aa 822–893). Exposure time for the autoradiogram was 3 h at room temperature. The bottom panel shows 20% input of in vitro-translated protein. Exposure time for the autoradiogram was 30 min at room temperature. Deletion of the last two EF hands, including the three terminal amino acids, or deletion of the three terminal amino acids alone, abolished binding to the PDZ domain (lanes 2 and 3). (D) Autoradiogram of  $^{35}\text{S}$  methionine-labeled proteins after coprecipitation with GST-PDZ glutathione resin. Lane 1, full-length  $\alpha$ -actinin 2; lane 2,  $\alpha$ -actinin 2 deleted for the three COOH-terminal amino acids (actinin-del3); lane 3 and 4, 20% input of in vitro-translated full-length  $\alpha$ -actinin 2 and actinin-del3 proteins. Exposure time for the autoradiogram was 3 h at room temperature.



$\alpha$ -actinin 2 (Xia et al., 1997). There are three L residues in the corresponding region of the Cypher PDZ domain: L76, 78, and 80. We mutated each of the three L residues to K individually and tested the interaction of each mutant Cypher with  $\alpha$ -actinin 2. Mutation of either L76 or L80 to K significantly reduced binding of the Cypher PDZ domain to  $\alpha$ -actinin 2, and mutation of L78 to K completely abolished the binding (Fig. 6). This in vitro biochemical result was confirmed by transfection studies in rat neonatal cardiomyocytes, in which a GFP-L78K fusion peptide no longer colocalized with  $\alpha$ -actinin (Fig. 5).

#### The COOH-terminal three amino acids of $\alpha$ -actinin 2 are essential for interaction between the Cypher PDZ domain and the COOH terminus of $\alpha$ -actinin 2

To define sites within  $\alpha$ -actinin 2 which bind to the PDZ domain, we made a series of  $\alpha$ -actinin 2 deletion constructs which were translated in vitro in the presence of [ $^{35}\text{S}$ ]methionine and subsequently assayed for binding to GST-PDZ fusion proteins. Results of these assays demonstrated that the COOH terminus of  $\alpha$ -actinin 2, containing four degenerate EF hands (aa 756–894), bound strongly to the Cypher PDZ domain (Fig. 7 B).

Examination of the  $\alpha$ -actinin 2 sequence revealed that the last three amino acids are SDL, which conform to the consensus PDZ binding motif S/T-X-V/I/L (Songyang et al., 1997). To test whether this SDL sequence within  $\alpha$ -actinin 2 is essential for its interaction with the Cypher PDZ domain, we made  $\alpha$ -actinin 2 mutants which contain the four EF hands but not the last three amino acids (4EF-del3, aa 756–891), the first two EF hands (EF1–2, aa 756–821), the last two EF hands (EF3–4, aa 822–894), and the full length

$\alpha$ -actinin 2 lacking the last three amino acids ( $\alpha$ -actinin 2-del3). Results from GST pull down assays demonstrated that EF3–4, containing the last two EF hands, retained the ability to bind to the PDZ domain, whereas EF1–2, lacking the last two EF hands, 4EF-del3, and  $\alpha$ -actinin 2-del3, lacking only the last three amino acids, no longer bound the PDZ domain (Fig. 7, C and D).

## Discussion

Congenital myopathies are a heterogeneous group of disorders with patients exhibiting muscle weakness at birth that is either nonprogressive or slowly progressive, and little or no evidence of myofiber necrosis and regeneration (Fardeau and Tome, 1994). On the other hand, congenital muscular dystrophies are a distinct group of disorders with progressive muscle weakness and obvious necrosis and regeneration of muscle fibers from birth (Dubowitz, 1989; Banker, 1994). Neonatal homozygous null mutants of cypher exhibit symptoms of muscle weakness, including decreased milk intake (dysphagia), minimal limb motility, and respiratory distress. However, no necrosis and regeneration of muscle fibers was observed in day 1 striated muscle. These observations suggest that cypher null mutants have a severe form of congenital myopathy, not congenital muscular dystrophy. *Cypher*<sup>-/-</sup> mice also display symptoms of heart failure, exhibiting both right and left ventricular dilation. We hypothesize that mutations within the human *cypher/ZASP* gene could result in human congenital myopathies with cardiac involvement.

To perform force-generating contraction, and to accommodate repetitive changes in cell geometry that occur during each contraction, striated muscle has evolved an abun-



dant and highly specialized cytoskeleton (Chen and Chien, 1999). Contractions of muscle cells enforce constant mechanical stress on the cell as a whole, and in particular on the Z-line due to its unique structural role. Abnormal Z-line structure was seen in sections from actively contracting skeletal and cardiac muscle in *cypher*<sup>-/-</sup> mutants. In contrast, sections of noncontracting embryonic diaphragm muscle in *cypher*<sup>-/-</sup> mutants exhibited normal Z-line structure. These observations suggest that Cypher is not required for the formation of protein complexes at the Z-line or sarcomerogenesis, but is essential for maintaining the structural integrity of the Z-line during the stress of contraction. In concert with our *in vitro* studies, these results reinforce the suggestion that Cypher functions as an linker-strut at the Z-line.

Results of our transfection studies with truncated Cypher–GFP fusion proteins demonstrated that the non-PDZ domains of Cypher localize independently to the Z-line. Our previous data showed that these domains do not interact with  $\alpha$ -actinin 2, suggesting that they are interacting with additional Z-line components. The demonstration that Cypher interacts with more than one Z-line component substantiates the hypothesis that Cypher is serving as a linker at the Z-line. We are currently trying to identify additional binding partners of Cypher.

The PDZ domain of ZASP, a human orthologue of Cypher, interacts with the last 150 amino acids of  $\alpha$ -actinin 2, as demonstrated by yeast two-hybrid interaction assays (Faulkner et al., 1999). Our data from GST pull down assays confirmed this result and have further identified the COOH-terminal last three amino acids of  $\alpha$ -actinin 2 as being required for this interaction. The PDZ domain of another member of the PDZ-LIM family, ALP, has been shown to interact with the spectrin repeats of  $\alpha$ -actinin 2 (Xia et al., 1997). However, the data presented did not exclude the possibility that the PDZ domain of ALP may also interact with the COOH terminus of  $\alpha$ -actinin 2.

We have also provided evidence that the ability of the Cypher PDZ domain to bind  $\alpha$ -actinin 2 is essential for localization of the PDZ domain to the Z-line. When transfected into cardiomyocytes, mutant PDZ domains G14A/F15A and L78K which no longer bound  $\alpha$ -actinin 2 *in vitro*, no longer colocalized with  $\alpha$ -actinin at the Z-line, but rather were localized diffusely throughout the cell. We have not yet performed similar studies with the L76K or L80K mutants, to determine whether their lower binding affinity for  $\alpha$ -actinin as detected in our binding studies is reflected in their cellular localization. As shown by previous investigators, *in vitro* binding data cannot always be extrapolated to cellular localization (Ojima et al., 1999).

ALP is one of the six members of the NH<sub>2</sub>-terminal PDZ domain and COOH-terminal LIM domain-containing protein family and is expressed predominantly in skeletal muscle and at much lower levels in cardiac and other tissues (Xia et al., 1997; Pomiès et al., 1999). *ALP* knockout mice have no apparent phenotype in skeletal muscles (Jo et al., 2001). However, some *ALP* knockouts display mild right ventricular dilation and cardiac dysfunction (Pashmforoush et al., 2001). It is of interest to note that expression of *ALP* and *cypher* overlaps at the Z-line in skeletal muscle, suggesting that Cypher may be able to compensate for ALP in skeletal

muscle. Within the heart, however, *ALP* expression is predominantly in right ventricle during development and restricted to the anterior-ventral segment of the RV/conotruncal region in adult heart (Pashmforoush et al., 2001). In contrast, *cypher* is expressed exclusively and uniformly in skeletal and cardiac muscle. In adult cardiomyocytes, ALP localizes predominantly to intercalated discs, whereas Cypher is evenly localized to the Z-lines, suggesting distinct functions for Cypher and ALP in heart (Zhou et al., 1999; Pashmforoush et al., 2001).

## Materials and methods

### Gene targeting

A genomic *cypher* fragment was isolated from a mouse 129svj genomic DNA library (Stratagene). PCR-based mutagenesis was used to convert the 1-kb pair fragment between three base pairs 5' of translational start codon ATG and intron 1 Hind III site into an XhoI site (Fig. 1 A). The deleted 1-kb fragment contained part of exon 1 and part of intron 1. LacZ and pGKneo-tk cassettes were inserted into the XhoI site. The linearized construct was electroporated into R1 ES cells. G418-resistant ES clones were screened for homologous recombination by Southern blotting with the probe as indicated in Fig. 1 A. Chimeric males were tested for germ-line transmission of the agouti coat phenotype of 129-derived ES cells by crossing with Black Swiss female breeders (Chen et al., 1998a,b). Total protein extracts were prepared (Chen et al., 1998b) from single postnatal day 1 heart ventricles, of which 25% were subjected to Western blotting analysis with Cypher polyclonal antibodies (Zhou et al., 1999) and tropomyosin monoclonal antibody (Chen et al., 1998b).

### Whole-mount X-gal staining of cypher transgenic embryos

For whole-mount LacZ expression analysis, transgenic embryos were fixed and stained using standard methods (Ross et al., 1996; Chu et al., 2000). Whole embryos or tissues were analyzed and photographed on a ZEISS SV-6 dissecting microscope with a Nikon C-mount 35 mm camera.

### TEM

Samples were processed for TEM as described (Chen et al., 1998b).

### Plasmid construction

Plasmids containing distinct parts of mouse  $\alpha$ -actinin 2, including the actin-binding domain, Spectrin repeats, or EF hands (Zhou et al., 1999), were generated by PCR using Pfu DNA polymerase (Stratagene) followed by cloning into pcDNA3FLAG (Zhou et al., 1999). Mutant PDZ domains were generated via PCR-based mutagenesis followed by subcloning into pGEX-4T-1 (Amersham Pharmacia Biotech) or pEGFP-C1 (CLONTECH). Each plasmid was sequenced to ensure that no PCR errors had been introduced.

### GST fusion protein binding assay

The assay was performed as described previously (Zhou et al., 1999). Briefly, proteins were labeled with [<sup>35</sup>S]-methionine via the TNT-coupled reticulocyte lysate system (Promega). Each GST fusion protein (200 pmol) was purified from bacteria, bound to 20  $\mu$ l of glutathione-agarose beads, and washed with binding buffer. The beads were then resuspended in 400  $\mu$ l binding buffer. 5–10  $\mu$ l of *in vitro*-translated protein was adjusted to 100  $\mu$ l with binding buffer and added to 400  $\mu$ l of GST fusion protein beads. The mixture was then incubated with rotation for 4 h at 4°C, and beads were washed six times with 100  $\mu$ l of binding buffer.

### Transfection of rat neonatal cardiomyocytes

Rat neonatal cardiomyocytes were prepared using a percoll gradient as described previously (Sheng et al., 1997). Isolated cells were plated on laminin-coated chamber slides at 250,000 cells/chamber in plating medium. After overnight incubation, the medium was switched to 10% horse serum and 5% fetal bovine serum for ~4 h before calcium-phosphate-mediated transfection (Zou and Chien, 1995). After 2 d of transfection, the cells were immunostained with antibodies or visualized for GFP.

### Immunohistochemistry

Transfected cardiomyocytes on chamber slides were rinsed twice with 1× PBS for 5 min, fixed in 4% paraformaldehyde for 10 min and washed with 1× PBS briefly followed by washing with 1× PBS for 5 min twice. Cells



were permeabilized and blocked with 1% BSA, 1% FBS, 0.3% Triton X-100 in 1× PBS for 30 min followed by incubation with 1:200 dilution of antisarcomeric  $\alpha$ -actinin antibody (Sigma-Aldrich) in 1% BSA, 1% FBS, 0.1% Tween-20 in PBS for 1 h. After washing for 5 min three times with 1× PBS, goat anti-mouse Cy3 antibody (Sigma-Aldrich) with a final dilution of 1:100 was added and incubated in 1% BSA, 1% FBS, 0.1% Tween-20 in PBS for 1 h. Slides were washed six times for 5 min with 1× PBS, then washed one time for 5 min with water, dried, and mounted with Gelvatol plus 2.5% DABCO (Zou and Chien, 1995). Slides were visualized on a ZEISS Axiovert 135 fluorescence microscope and photographed using a 63× Plan-apochromat objective (ZEISS).

We thank Andrea Thorn and Norma Prades for technical assistance.

This work was supported by a grant from the Muscular Dystrophy Association (J. Chen). P.H. Chu was supported by a grant from Chung Gang Memorial Hospital at Taiwan.

Submitted: 23 July 2001

Revised: 28 September 2001

Accepted: 1 October 2001

## References

- Anversa, P., G. Olivetti, P.G. Bracchi, and A.V. Loud. 1981. Postnatal development of the M-band in rat cardiac myofibrils. *Circ. Res.* 48:561–568.
- Banker, B.Q. 1994. The congenital muscular dystrophies. In *Myology*. A.G. Engel and C. Franzini-Armstrong, editors. McGraw-Hill, Inc., New York. 1275–1289.
- Beggs, A.H., T.J. Byers, J.H. Knoll, F.M. Boyce, G.A. Bruns, and L.M. Kunkel. 1992. Cloning and characterization of two human skeletal muscle alpha-actinin genes located on chromosomes 1 and 11. *J. Biol. Chem.* 267:9281–9288.
- Chen, J., and K.R. Chien. 1999. Complexity in simplicity: monogenic disorders and complex cardiomyopathies. *J. Clin. Invest.* 103:1483–1485.
- Chen, J., S.W. Kubalak, and K.R. Chien. 1998a. Ventricular muscle-restricted targeting of the RXRalpha gene reveals a non-cell-autonomous requirement in cardiac chamber morphogenesis. *Development*. 125:1943–1949.
- Chen, J., S.W. Kubalak, S. Minamisawa, R.L. Price, K.D. Becker, R. Hickey, J. Ross, Jr., and K.R. Chien. 1998b. Selective requirement of myosin light chain 2v in embryonic heart function. *J. Biol. Chem.* 273:1252–1256.
- Chu, P.H., P. Ruiz-Lozano, Q. Zhou, C. Cai, and J. Chen. 2000. Expression patterns of FHL/Slim family members suggest important functional roles in skeletal muscle and cardiovascular system. *Mech. Dev.* 95:259–265.
- Djinovic-Carugo, K., P. Young, M. Gautel, and M. Saraste. 1999. Structure of the  $\alpha$ -actinin rod: molecular basis for cross-linking of actin filaments. *Cell*. 98:537–546.
- Doyle, D.A., A. Lee, J. Lewis, E. Kim, M. Sheng, and R. MacKinnon. 1996. Crystal structures of a complexed and peptide-free membrane protein-binding domain: molecular basis of peptide recognition by PDZ. *Cell*. 85:1067–1076.
- Dubowitz, V. 1989. Congenital muscular dystrophy. In *Color Atlas of Muscle Disorders in Childhood*. V. Dubowitz, editor. Year Book Medical Pub., Chicago. 52–65.
- Fardeau, M., and F.M.S. Tome. 1994. Congenital Myopathies. In *Myology*. A.G. Engel and C. Franzini-Armstrong, editors. McGraw-Hill, Inc., New York. 1487–1532.
- Faulkner, G., A. Pallavicini, E. Formentin, A. Comelli, C. Ievolella, S. Trevisan, G. Bortoletto, P. Scannapieco, M. Salamon, V. Mouly, et al. 1999. ZASP: a new Z-band alternatively spliced PDZ-motif protein. *J. Cell Biol.* 146:465–475.
- Goldstein, M.A., J.P. Schroeter, and L.H. Michael. 1991. Role of the Z band in the mechanical properties of the heart. *FASEB J.* 5:2167–2174.
- Jo, K., B. Rutten, R.C. Bunn, and D.S. Bredt. 2001. Actinin-associated LIM protein-deficient mice maintain normal development and structure of skeletal muscle. *Mol. Cell Biol.* 21:1682–1687.
- Kiess, M., B. Scharm, A. Aguzzi, A. Hajnal, R. Klemenz, I. Schwarte-Waldhoff, and R. Schäfer. 1995. Expression of ril, a novel LIM domain gene, is down-regulated in Hras-transformed cells and restored in phenotypic revertants. *Oncogene*. 10:61–68.
- Kuroda, S., C. Tokunaga, Y. Kiyohara, O. Higuchi, H. Konishi, K. Mizuno, G.N. Gill, and U. Kikkawa. 1996. Protein-protein interaction of zinc finger LIM domains with protein kinase C. *J. Biol. Chem.* 271:31029–31032.
- Luther, P.K. 2000. Three-dimensional structure of a vertebrate muscle Z-band: implications for titin and alpha-actinin binding. *J. Struct. Biol.* 129:1–16.
- Ojima, K., Z.X. Lin, Z.Q. Zhang, T. Hijikata, S. Holtzer, S. Labeit, H.L. Sweeney, and H. Holtzer. 1999. Initiation and maturation of I-Z-I bodies in the growth tips of transfected myotubes. *J. Cell Sci.* 112:4101–4112.
- Pashmforoush, M., P. Pomies, K.L. Peterson, S. Kubalak, J.J. Ross, A. Hefti, U. Aebi, M. Beckerle, and K.R. Chien. 2001. Adult mice deficient in actinin-associated LIM-domain protein reveal a developmental pathway for right ventricular cardiomyopathy. *Nat. Med.* 7:591–597.
- Pomies, P., T. Macalma, and M.C. Beckerle. 1999. Purification and characterization of an alpha-actinin-binding PDZ-LIM protein that is up-regulated during muscle differentiation. *J. Biol. Chem.* 274:29242–29250.
- Ross, R.S., S. Navankasattusas, R.P. Harvey, and K.R. Chien. 1996. An HF-1a/HF-1b/MEF-2 combinatorial element confers cardiac ventricular specificity and established an anterior-posterior gradient of expression. *Development*. 122:1799–1809.
- Sheng, Z., K. Knowlton, J. Chen, M. Hoshijima, J.H. Brown, and K.R. Chien. 1997. Cardiotrophin 1 (CT-1) inhibition of cardiac myocyte apoptosis via a mitogen-activated protein kinase-dependent pathway. Divergence from downstream CT-1 signals for myocardial cell hypertrophy. *J. Biol. Chem.* 272:5783–5791.
- Songyang, Z., A.S. Fanning, C. Fu, J. Xu, S.M. Marfatia, A.H. Chishti, A. Crompton, A.C. Chan, J.M. Anderson, and L.C. Cantley. 1997. Recognition of unique carboxyl-terminal motifs by distinct PDZ domains. *Science*. 275:73–77.
- Wang, H., D.C. Harrison-Shostak, J.J. Lemasters, and B. Herman. 1995. Cloning of a rat cDNA encoding a novel LIM domain protein with high homology to rat RIL. *Gene*. 165:267–271.
- Wu, R.Y., and G.N. Gill. 1994. LIM domain recognition of a tyrosine-containing tight turn. *J. Biol. Chem.* 269:25085–25090.
- Xia, H., S.T. Winokur, W.L. Kuo, M.R. Altherr, and D.S. Bredt. 1997. Actinin-associated LIM protein: identification of a domain interaction between PDZ and spectrin-like repeat motifs. *J. Cell Biol.* 139:507–515.
- Young, P., C. Ferguson, S. Bafielos, and M. Gautel. 1998. Molecular structure of the sarcomeric Z-disk: two types of titin interactions lead to an asymmetrical sorting of alpha-actinin. *EMBO J.* 17:1614–1624.
- Zhou, Q., P. Ruiz-Lozano, M.E. Martone, and J. Chen. 1999. Cypher, a striated muscle-restricted PDZ and LIM domain-containing protein, binds to alpha-actinin-2 and protein kinase C. *J. Biol. Chem.* 274:19807–19813.
- Zou, Y., and K.R. Chien. 1995. EFIA/YB-1 is a component of cardiac HF-1A binding activity and positively regulates transcription of the myosin light-chain 2v gene. *Mol. Cell Biol.* 15:2972–2982.